

Lidocaine Increases Intracellular Sodium Concentration through Voltage-dependent Sodium Channels in an Identified *Lymnaea* Neuron

Shin Onizuka, M.D.,* Toshiharu Kasaba, M.D.,† Toshiro Hamakawa, M.D.,‡ Shoichiro Ibusuki, M.D.,* Mayumi Takasaki, M.D., Ph.D.§

Background: The local anesthetic lidocaine affects neuronal excitability in the central nervous system; however, the mechanisms of such action remain unclear. The intracellular sodium concentration ($[Na^+]_i$) and sodium currents (INa) are related to membrane potential and excitability. Using an identifiable respiratory pacemaker neuron from *Lymnaea stagnalis*, the authors sought to determine whether lidocaine changes $[Na^+]_i$ and membrane potential and whether INa is related to these changes.

Methods: Intracellular recording and sodium imaging were used simultaneously to measure membrane potentials and $[Na^+]_i$, respectively. Measurements for $[Na^+]_i$ were made in normal, high- Na^+ , and Na^+ -free salines, with membrane hyperpolarization, and with tetrodotoxin pretreatment trials. Furthermore, changes of INa were measured by whole cell patch clamp configuration.

Results: Lidocaine increased $[Na^+]_i$ in a dose-dependent manner concurrent with a depolarization of the membrane potential. In the presence of high- Na^+ saline, $[Na^+]_i$ increased and the membrane potential was depolarized; the addition of lidocaine further increased $[Na^+]_i$, and the membrane potential was further depolarized. In Na^+ -free saline or in the presence of tetrodotoxin, lidocaine did not change $[Na^+]_i$. Similarly, hyperpolarization of the membrane by current injections also prevented the lidocaine-induced increase of $[Na^+]_i$. In the patch clamp configuration, membrane depolarization by lidocaine led to an inward sodium influx. A persistent reduction in membrane potential, resulting from lidocaine, brings the cell within the window current of INa where sodium channel activation occurs.

Conclusion: Lidocaine increases intracellular sodium concentration and promotes excitation through voltage-dependent sodium channels by altering membrane potential in the respiratory pacemaker neuron.

LIDOCAINE is widely used for regional anesthesia and postoperative pain relief, and these effects involve the blockade of voltage-dependent sodium channels. When used even within a clinical range, focally applied lidocaine can enter the central nervous system to affect its function. In a classic theory presented in most textbooks, this excitation exerted by local anesthetics is thought to be the result of an initial blockade of inhibitory pathways in the cerebral cortex.^{1,2} On the other

hand, the local anesthetic-induced excitation is believed to result from an increase in the excitability of individual neurons.^{3,4} In any case, the precise mechanisms remain unclear.

Intracellular sodium concentration ($[Na^+]_i$) and sodium currents (INa) are prime indicators of neuronal excitability. Depolarizing inputs alter membrane potential and open voltage-dependent sodium channels. In addition, the activation of voltage-dependent sodium channels in neurons increases sodium currents and excites neurons.^{5,6} In this process, Na^+ influx occurs from the extracellular space *via* sodium-potassium or sodium-calcium exchangers and by the activation of voltage-gated sodium channels.^{7,8} Rodeau *et al.*⁹ reported that 10 mM procaine induces inward INa and depolarizes the membrane potential through an inward current of procaine itself. On the other hand, Castaneda-Castellanos *et al.*¹⁰ reported that lidocaine (0.1 mM) maintains the voltage-dependent sodium channels in an open state, resulting in Na^+ influx and neuronal excitability. If lidocaine increases inward INa or stabilizes the open state of voltage-dependent sodium channels, lidocaine is also expected to change $[Na^+]_i$. However, there are no published reports to show that local anesthetics alter $[Na^+]_i$ concentration.

In this study, we isolated the identified neuron right pedal dorsal 1 (RPd1) from the fresh water snail *Lymnaea stagnalis*. This giant neuron was used because it is one of the pacemaker neurons involved in respiratory pattern generation.¹¹ This pacemaker neuron, like other respiratory pacemaker neurons, has a slowly inactivating component of the sodium current and can produce spontaneous action potentials continuously.¹²⁻¹⁴ There are few reports of the effect of local anesthetics on respiratory pacemaker neurons, because to detect, identify, and isolate respiratory pacemaker neurons in the central nervous system is difficult in mammalian preparations. In contrast, it is easy to isolate the snail brain and remove individual neurons. An *in vitro* isolated neuron is devoid of other confounding inputs such as other neurons and glial cells, making it possible to observe $[Na^+]_i$ purely and clearly. Moreover, in the absence of an extensive neuritic arbor, this neuron poses fewer current clamp challenges. Ion channels, including voltage-dependent sodium channels, which are similar to those of humans and can be blocked by tetrodotoxin selectively, have been previously investigated in RPd1.^{15,16} Identified *Lymnaea* neurons have in the past been ex-

* Instructor in Anesthesiology, † Associate Professor of Anesthesiology, ‡ Assistant Professor of Anesthesiology, § Professor of Anesthesiology.

Received from the Department of Anesthesiology, Miyazaki Medical College, University of Miyazaki, Kiyotake, Miyazaki, Japan. Submitted for publication August 6, 2003. Accepted for publication March 5, 2004. Supported in part by Grant-in-Aid No. 12770828 for Scientific Research (A) from the Ministry of Education, Science and Technology of Japan, Tokyo, Japan.

Address reprint requests to Dr. Onizuka: Department of Anesthesiology, Miyazaki Medical College, University of Miyazaki, Kiyotake-Cho, Miyazaki, 889-1692, Japan. Address electronic mail to: onizuka@shaw.ca. Individual article reprints may be purchased through the Journal Web site, www.anesthesiology.org.

tensively used to define the mechanisms by which both inhalation and intravenous anesthetics affect neuronal properties and synaptic transmission in the nervous system.¹⁷⁻¹⁹

In individual RPeD1 neurons, the changes of membrane potential and $[Na^+]_i$ before and after lidocaine administration were measured simultaneously by intracellular microelectrode recording and sodium-binding benzofuran isophthalate (SBFI) imaging. Furthermore, to investigate the relation between $[Na^+]_i$ and membrane potential, the changes of INa before and after lidocaine perfusion were measured by whole cell patch clamp (voltage clamp) configuration.

Materials and Methods

Animal and Cell Culture

All animal experiments were approved by the Animal Care Committee of Miyazaki Medical College (Kiyotake, Miyazaki, Japan). The cell culture procedures were adopted from Syed *et al.*¹¹ Specifically, we used individually identifiable RPeD1 neurons from laboratory-raised *L. stagnalis* (fresh water snail) at room temperature. For this study, 2- to 3-month-old snails (shell length, 20–30 mm) were selected. Snails were deshelled and transferred to a sterile dissection dish in antibiotic normal saline (150 μ g/ml Gentamicin [G3632; Sigma Chemical Co., St. Louis, MO] in normal *Lymnaea* saline: 51.3 mM NaCl, 1.7 mM KCl, 4.1 mM $CaCl_2$, 1.5 mM $MgCl_2$, 5.0 mM HEPES, pH 7.9). The central ganglionic rings were isolated using standard dissection procedures and subsequently pinned to the silicone rubber base of a tissue culture plate. The outer connective tissue of the ganglia was removed before enzymatic treatment. Ganglia were treated in defined medium (serum-free 50% Leibovitz L-15 medium [GIBCO-BRL Life Technologies, Burlington, Ontario, Canada] with added inorganic salts, 20 μ g/ml gentamycin, pH 7.9) for 25 min with 0.2% trypsin (type III; Sigma Chemical Co.). Subsequently, ganglia were also treated with 0.2% soybean trypsin inhibitor (Sigma Chemical Co.) for 15 min in the defined medium. Before removal of identified neurons, the inner connective tissue sheath was dissected with fine forceps from the ganglia. Neurons were removed by gentle suction with a siliconized, microforge fine-polished pipette with an outside diameter of 1.5 mm (IB-150 F; WPI, Sarasota, FL), and then these neurons were maintained in a high-osmolarity medium containing 30 mM glucose. After this, neurons were transferred to poly-L-lysine-coated culture dishes (Falcon Plastics, Los Angeles, CA) with 3 ml of the defined medium.

Intracellular Recording and $[Na^+]_i$ Imaging

The following neuronal activity was monitored using conventional intracellular recording. A glass microelec-

trode, outside diameter of 1.0 mm (GC100-10; CEI, London, England) was filled with a saturated solution of K_2SO_4 , yielding a tip resistance of 20–60 M Ω . A neuron was observed under an inverted microscope (TE-300; Nikon, Tokyo, Japan) and impaled by a microelectrode using a manipulator (MM 202; M 204, Narishige, Japan). Electrical signals were amplified (IR-283; Cygnus Technologies, Delaware Water Gap, PA), displayed on an oscilloscope (VC-11; Nihon Kohden, Tokyo, Japan), and stored on computer (G4; Apple Computer Inc., Cupertino, CA) through an A/D converter (Powerlab; ADInstruments, Colorado Springs, CO) and a thermal alley recorder (RTA1200; Nihon Kohden).

For the measurement of $[Na^+]_i$, the radiometric fluorescent indicator, an acetoxymethyl ester form of sodium-binding benzofuran isophthalate (SBFI-AM) (Molecular Probes, Eugene, OR) was used. SBFI-AM, 1 mM, in dimethyl sulfoxide (DMSO) was mixed with the defined medium containing the neuron at a volume of 0.1%. After incubation at 20°C for 60 min, this defined medium was removed, and the neuron was suspended in normal saline for 1 h to take out hydrolysis of AM esters and diacetates. Measurements were made by exciting this indicator dye at 340 nm, where fluorescence is particularly sensitive to the sodium ion concentration, and 390 nm, where is very close to the isosbestic point.²⁰⁻²² Therefore, the intensity of intracellular SBFI fluorescence was measured at two quickly alternating excitation wavelengths (340/390 nm) and continuously recorded at 510 nm by an inverted fluorescent microscope (TE-300), a cooled high-speed charge-coupled device video camera (C-6970; Hamamatsu Photonics, Hamamatsu, Japan), and a fluorescence imaging system (Argus-Hisca; Hamamatsu Photonics). The exposure time for a single image was 159 ms, resulting in a total time of 600 ms needed for a 340/390-nm pair image. Background fluorescent images were subtracted before analysis.

In Vivo Calibration for $[Na^+]_i$

Two fluorescence ratios with SBFI were converted into using the calibration curve for RPeD1 *in vivo*.²³⁻²⁵ The calibration curve for $[Na^+]_i$ was constructed by plotting the fluorescence ratio *versus* Na^+ concentration of the calibration solutions (fig. 1). To equilibrate the $[Na^+]_i$ with extra ($[Na^+]_o$), 30 min before the experiment, 10 μ M of the Na^+ ionophore gramicidin D (ICN Biomedicals, Inc., Costa Mesa, CA) was added, and then RPeD1 neurons were exposed to Na^+ -free concentration saline with gramicidin D solution for 30 min. Fluorescent image pairs were taken, and then RPeD1 neurons were exposed to salines of increasing sodium concentration (1, 25, 50, 100, 150 mM) for 10 min each. Image pairs were taken again at the end of each exposure.

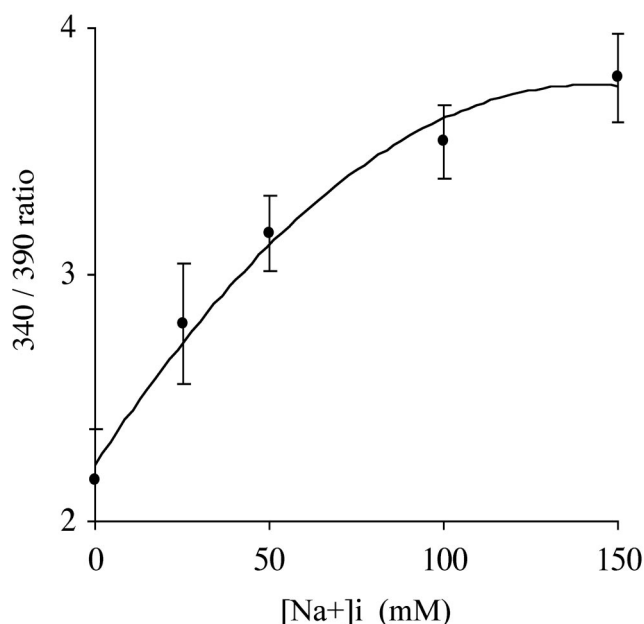


Fig. 1. The *in vivo* calibration curve of sodium-binding benzo-furan isophthalate 340/390-nm intensity ratio versus intracellular sodium concentrations ($[Na^+]_i$) in right pedal dorsal 1 neuron. Each value represents mean \pm SEM; $n = 10$.

Experimental Procedure for Intracellular Recording and $[Na^+]_i$ Imaging

Neurons were divided into five trials: normal saline, high- Na^+ saline, Na^+ -free saline, membrane hyperpolarization, and tetrodotoxin (Sankyo, Tokyo, Japan; 30 μM) pretreatment. For the membrane hyperpolarization trials, the membrane potential was held at -80 mV by current injection 2 min before lidocaine perfusion. In the high- Na^+ saline trials, high- Na^+ saline (103 mM NaCl, 1.7 mM KCl, 4.1 mM $CaCl_2$, 1.5 mM $MgCl_2$, 5.0 mM HEPES, pH 7.9) was used as the extracellular fluid. In the Na^+ -free saline trials, Na^+ -free saline (0 mM NaCl, 50 mM *N*-methyl-D-glucamine, 1.7 mM KCl, 4.1 mM $CaCl_2$, 1.5 mM $MgCl_2$, 5.0 mM HEPES, pH 7.9) was used. In the normal saline, membrane hyperpolarization, and tetrodotoxin pretreatment trials, normal saline was used.

In the normal saline trials, lidocaine (0.01, 0.1, and 1 mM) was perfused into the culture dish after measurements of baseline values. In the high- Na^+ saline, Na^+ -free saline, membrane hyperpolarization, and tetrodotoxin pretreatment trials, 1 mM lidocaine was perfused. In the tetrodotoxin pretreatment trials, tetrodotoxin (30 μM) was perfused for 4–6 min before lidocaine perfusion.

In the normal saline trials, membrane potential and $[Na^+]_i$ were measured for 5 min after each dose of lidocaine. In the high- Na^+ saline and the Na^+ -free saline trials, the normal salines were changed to either high- Na^+ or Na^+ -free saline at 2 min, and membrane potential and $[Na^+]_i$ were measured for 7 min after lidocaine administration. In the normal saline and membrane hyperpolarization trials, the baseline values were collected

during the 4 min before lidocaine perfusion (at 0 min in the figures). In the high- Na^+ saline, Na^+ -free saline, and tetrodotoxin pretreatment trials, the baseline values were measured 2 min before lidocaine perfusion (at 0 min in the figures). In each trial, the membrane potential was measured relative to the resting membrane potential of -60 mV in RPeD1.

Whole Cell Patch Clamp Recordings

Whole cell voltage clamp recordings in RPeD1 neurons^{26,27} were made using an EPC9 amplifier (HEKA elektronik, Lambrecht, Germany). Patch electrodes (tip diameter adjusted to 1.0 μm , resistance of 1–3 M Ω) were pulled from glass tubing (outside diameter of 1.5 mm) with no filament (PG-150T-7.5; Warner Instrument, Hamden, CT) on a vertical pipette puller (Kopf 750, Tujunga, CA). For experiment control and data acquisition, an A/D and D/A converter interface board (PCI-16; HEKA elektronik) was inserted into a personal computer (G4). Data acquisition and analysis were performed using Pulse software (version 8.66; HEKA elektronik). The current was filtered at 1 kHz using a four-pole Bessel filter and digitized at a sampling frequency of 20 kHz. To study INa, pipettes were filled with filtered (0.22- μm filter) cesium pipette solution consisting of 50 mM CsCl, 5 mM EGTA, 5 mM $MgCl_2$, 10 mM HEPES, 2 mM ATP-Mg, and 0.1 mM GTP-Tris, and the pH was adjusted to 7.4 (with CsOH). The bath solution consisted of 40 mM NaCl, 10 mM TEACl, 4.0 mM $MgCl_2$, 1.0 mM $CaCl_2$, 1.0 mM 4-aminopyridine, 1.0 mM $CdCl_2$, and 10 mM HEPES (pH 7.9).^{26,27} All experiments were performed at room temperature (20°–22°C). After obtaining a gigohm seal, the series resistance was compensated approximately 70–80% using the series resistance compensation of the pulse software, and the final series resistance level was compensated under 1 M Ω . The leak currents were subtracted by leak compensation within the pulse software for each experiment.

Experimental Procedure for Whole Cell Patch Clamp Recordings

In whole cell voltage clamp recordings, neurons were divided into three groups: control, 0.1, and 1 mM lidocaine perfusion groups. Currents were measured 6 min after each dose of lidocaine. The current-voltage curve, steady state activation curve, and steady state inactivation curve were plotted.

Current-Voltage Curve

For the current-voltage curve, INa was measured in response to 10-mV, 20-ms steps from a holding potential of -120 mV (1 s) and 10-mV incremental steps to potentials between -80 and $+40$ mV.^{26,27} Currents were normalized to the maximum in control and plotted as a function of membrane potential.

Steady State Activation Curve

For the steady state activation curve, peak I_{Na} was measured in response to 20-ms, 10-mV incremental depolarizing steps from -120 to $+40$ mV from a holding potential of -120 mV for 1 s. From the peak I_{Na} , the conductance values (G) were calculated according to the equation $G = I_{Na}/(V - E_{Na})$, where I_{Na} was the peak Na^+ current measured at each membrane potential (V), and E_{Na} is the reversal potential estimated by the current-voltage curve.²⁸ Calculated G values were normalized to the maximum of the control or to the maximum of each group and plotted as a function of membrane potential. Plots were fitted to Boltzmann relations of the form $y = G_{min} + (G_{max} - G_{min})/[1 + \exp[(V - V_{50})/K]]$, where y is normalized G_{Na} , G_{min} is the G of baseline, G_{max} is the G of maximum, V is each membrane potential, V_{50} is the membrane potential at which conductance is halfway between G_{min} and G_{max} , and K is the slope factor.^{10,28,29}

Steady State Inactivation Curve

For the steady state inactivation curve, the membrane potential was prepulsed from -120 to 40 mV at 10-mV increments for 5 s. I_{Na} was measured with a 20-ms test pulse to -10 mV. Currents were normalized to the maximum in control and plotted as a function of prepulse potential. Plots were fitted to Boltzmann relations of the form $y = I_{min} + (I_{max} - I_{min})/[1 + \exp[(V - V_{50})/K]]$, where y is normalized I_{Na} of the maximum in control or in each group, I_{min} is the I_{Na} of baseline, I_{max} is the I_{Na} of maximum, V is each prepulse potential, V_{50} is the membrane potential at which conductance is halfway between I_{min} and I_{max} , and K is a slope factor.^{10,28,29} In steady state activation and inactivation curves, analyses were performed using Kaleida graph (version 3.52; Synergy Software, Reading, PA).

Statistical Analysis

Results are expressed as mean \pm SEM. The results of repeated measurements in each dose in each group of trials were analyzed by repeated-measurement one-way analysis of variance, followed by the Scheffé test. Among the three doses of lidocaine in the normal saline trials and among the high- Na^+ saline, Na^+ -free saline, hyperpolarized, and tetrodotoxin pretreatment trials, the three groups in the current-voltage curve of whole cell patch clamp recordings were analyzed by analysis of variance, followed by the Scheffé test. Stat view (version 4.5; Abacus, Berkeley, CA) was used for these analyses. $P < 0.05$ was considered statistically significant.

Results

Intracellular Recording and $[Na^+]_i$ Imaging

Normal Saline Trials. To test whether lidocaine affects neuronal excitability and intracellular Na concen-

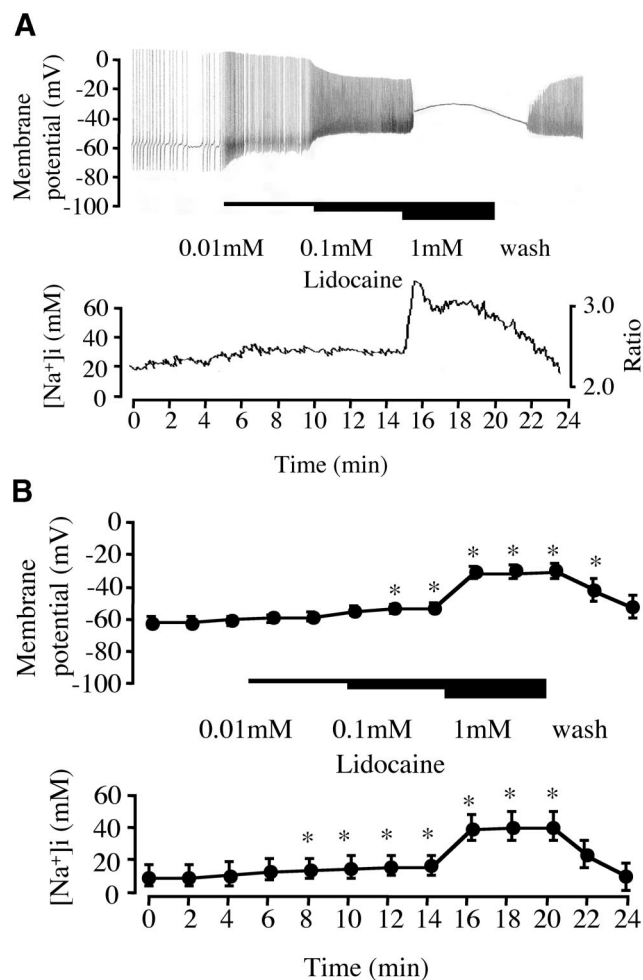


Fig. 2. (A) Simultaneous traces of membrane potential (top) ratio and intracellular sodium concentrations ($[Na^+]_i$) (bottom) in the normal saline trials. Lidocaine was perfused at 5 min (0.01 mM), 10 min (0.1 mM), and 15 min (1 mM). (B) Data of membrane potential (top) and $[Na^+]_i$ (bottom). Results are presented as mean \pm SEM; $n = 10$. * $P < 0.05$ compared with baseline values.

tration, intracellular activity of individually isolated neurons were monitored either in the absence or in the presence of lidocaine.

The mean values of the fluorescence ratio and $[Na^+]_i$ at resting membrane potential were 2.4 ± 0.1 and 9 ± 6 mM, respectively. There was no difference in the initial mean values of $[Na^+]_i$ before lidocaine or tetrodotoxin administration in each trial. Half of RPd1 neurons have spontaneous activity at resting membrane potentials.

Figure 2A shows experimental tracings of membrane potential and $[Na^+]_i$ before and after lidocaine administration. After lidocaine perfusion, $[Na^+]_i$ increased, and membrane potential depolarized. Soon after a high dose of lidocaine (1 mM), $[Na^+]_i$ increased, membrane potential continued to be depolarized, and action potential frequency increased (maximum frequency of action potentials: from 5 ± 5 to 37 ± 9 rate/min at 0.01 mM, to 80 ± 12 rate/min at 0.1 mM, and to 114 ± 21 rate/min at 1

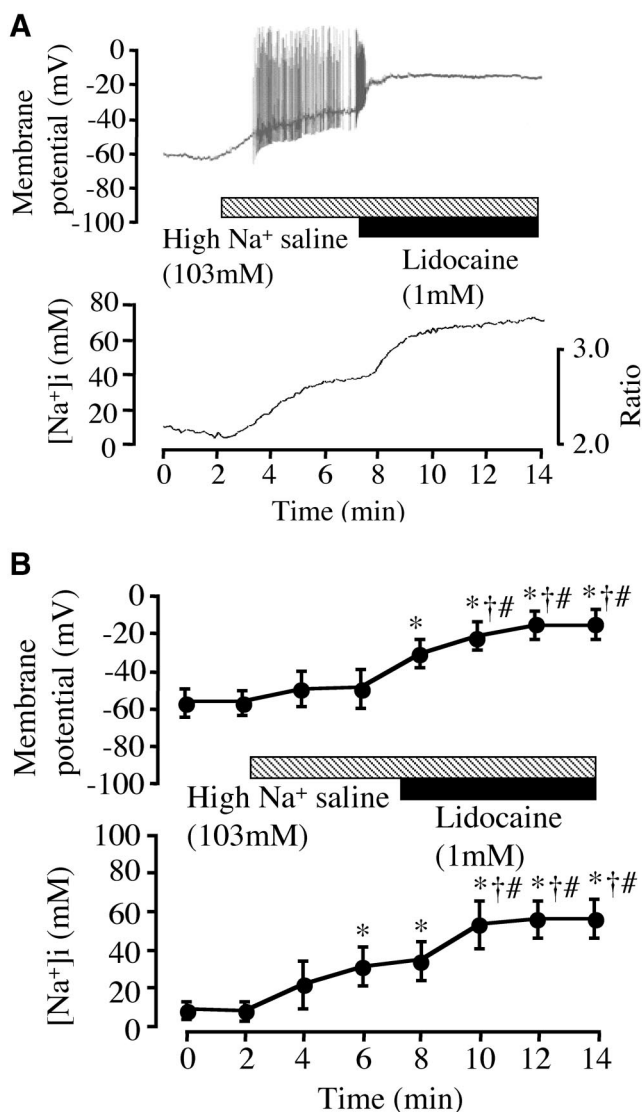


Fig. 3. (A) Simultaneous traces of membrane potential (top) and intracellular sodium concentrations ($[Na^+]_i$) (bottom) in the high- Na^+ saline trials. The normal saline was changed to high- Na^+ saline from 2 to 14 min. Lidocaine was perfused at 7 min (1 mM). (B) Data of membrane potential (top) and $[Na^+]_i$ (bottom) in the high- Na^+ saline. Results are presented as mean \pm SEM; $n = 9$. * $P < 0.05$ compared with baseline values. † $P < 0.05$ compared with high- Na^+ saline perfusion. # $P < 0.05$ compared with normal saline trials.

mm). However, this initial increase in action potential frequency was transient, lasting only a few seconds, followed by a flat membrane potential. In the normal saline trials, lidocaine significantly depolarized the membrane potential (from -59 ± 3 to -55 ± 3 mV at 0.01 mM, to -50 ± 3 mV at 0.1 mM, and to -21 ± 3 mV at 1 mM; fig. 2B). $[Na^+]_i$ was significantly increased at each lidocaine dose (from 9 ± 6 to 14 ± 6 mM at 0.01 mM, to 16 ± 6 at 0.1 mM, and to 39 ± 9 at 1 mM; fig. 2B). Both the depolarization of the membrane potential and the increase in $[Na^+]_i$ after lidocaine perfusion were dose dependent.

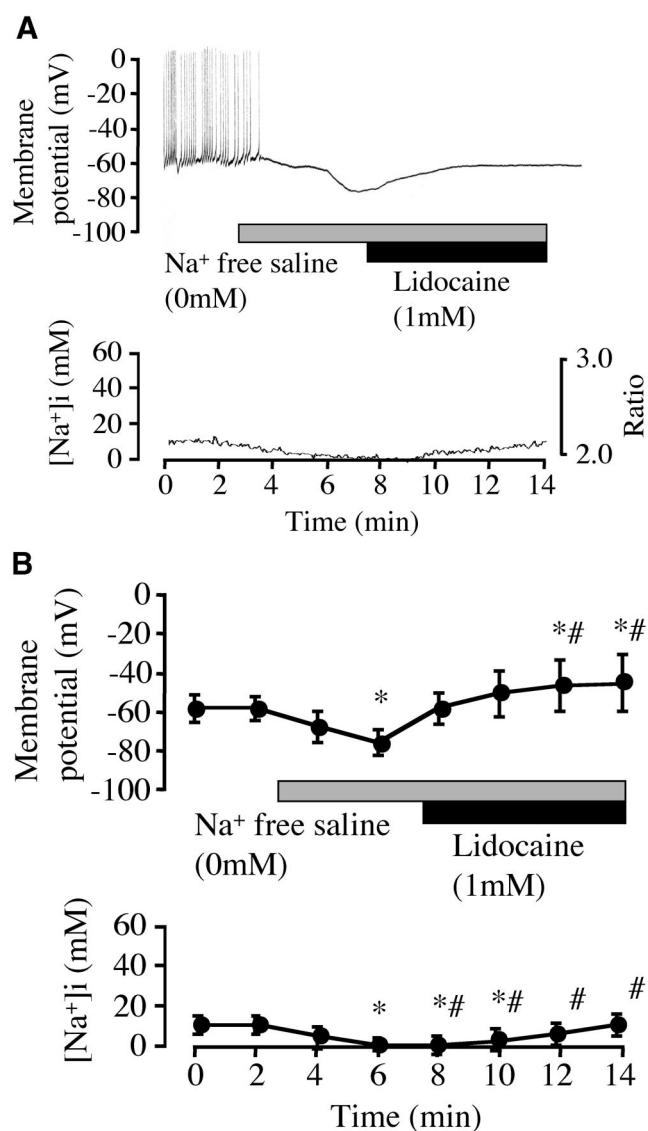


Fig. 4. (A) Simultaneous traces of membrane potential (top) and intracellular sodium concentrations ($[Na^+]_i$) (bottom) in the Na^+ free saline. The normal saline was changed to Na^+ free saline from 2 min to 14 min. Lidocaine was perfused at 7 min (1 mM). (B) The data of membrane potential (top) and $[Na^+]_i$ (bottom) in the Na^+ free saline. Results are presented as mean \pm SEM; $n = 9$. * $P < 0.05$ compared with baseline values. # $P < 0.05$ compared with normal saline trials.

High- Na^+ Saline Trials. The membrane potential and the $[Na^+]_i$ were stabilized for 2 min before high- Na^+ saline application, and also, these were allowed to stabilize in high- Na^+ saline 2 min before lidocaine application. High- Na^+ saline increased $[Na^+]_i$ and depolarized membrane potential. Subsequent application of lidocaine, in the presence of high- Na^+ saline, further increased $[Na^+]_i$ and also further depolarized the membrane. ($[Na^+]_i$: from 10 ± 3 to 59 ± 10 mM; membrane potentials: from -58 ± 6 to -14 ± 4 mV; fig. 3). The membrane potential and the intracellular sodium concentration after lidocaine perfusion were compared not

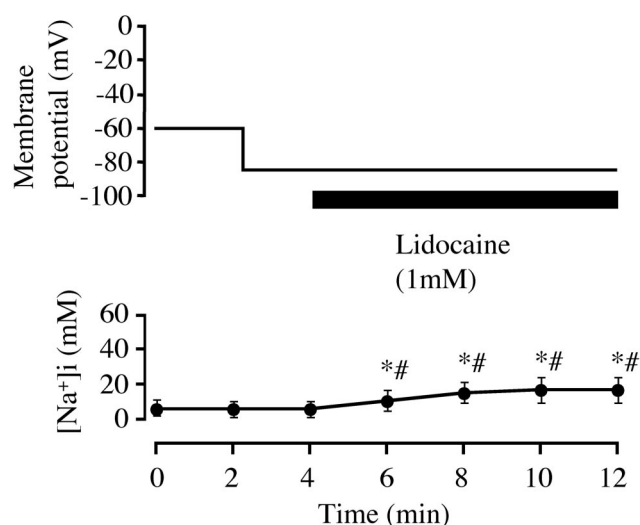


Fig. 5. Data of membrane potential (*top*) and intracellular sodium concentrations ($[Na^+]_i$) (*bottom*) in the membrane hyperpolarization trials. The membrane potential was hyperpolarized and voltage clamped from -60 mV to -80 mV at 2 min. Lidocaine (1 mM) was perfused at 4 min. Results are presented as mean \pm SEM; $n = 10$. * $P < 0.05$ compared with baseline values. # $P < 0.05$ compared with normal saline trials.

only with the data of control but also with the data after high- Na^+ saline perfusion during the same period.

Na^+ -free Saline Trials. In the Na^+ -free saline trials, the increase in $[Na^+]_i$ after lidocaine perfusion was significantly lower than that of normal saline trials (from 7 ± 4 to 5 ± 3 mM; fig. 4). Membrane potential was depolarized after lidocaine perfusion (from -58 ± 4 to -44 ± 14 mV), and this increase was significantly less than that of normal saline trials.

Membrane Hyperpolarization Trials. In the membrane hyperpolarization trials, where membrane potential was reduced from -60 mV to -80 mV, spontaneous action potentials ceased to occur. In the membrane hyperpolarization trials, the increase in $[Na^+]_i$ after lidocaine perfusion was significantly lower than that of normal saline trials (from 8 ± 4 to 17 ± 6 mM; fig. 5).

Tetrodotoxin Pretreatment Trials. Tetrodotoxin ($30 \mu M$) significantly suppressed the lidocaine-induced increase in $[Na^+]_i$ and membrane potential depolarization when compared with normal saline trials ($[Na^+]_i$: from 9 ± 2 to 11 ± 3 mM; membrane potentials: from -59 ± 2 to -56 ± 6 mV; fig. 6).

Whole Cell Patch Clamp Recordings

Characteristics of I_{Na} . In the presence of normal saline, the threshold for I_{Na} was -40 mV, and the maximum current response occurred at -10 mV, with the mean value at -1.73 ± 0.12 nA. The reversal potential of I_{Na} was $+22$ mV. The I_{Na} was blocked by $30 \mu M$ tetrodotoxin at all potentials.

Effects of Lidocaine on I_{Na} . Lidocaine decreased maximum current response of I_{Na} at -10 mV in a

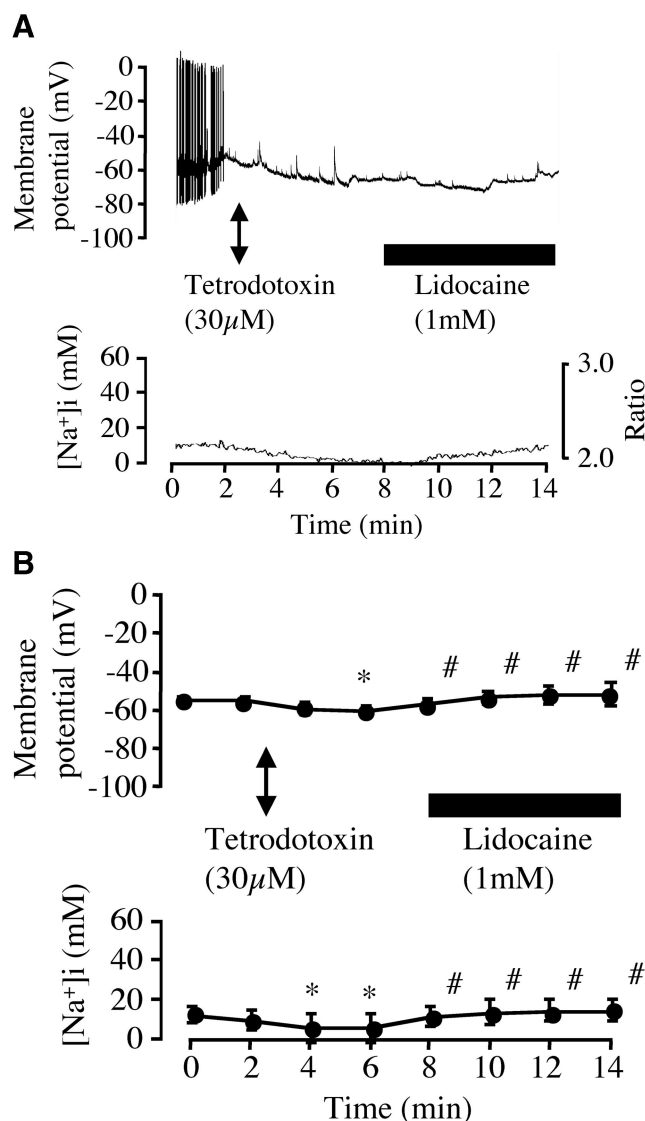


Fig. 6. (A) Simultaneous traces of membrane potential (*top*) and intracellular sodium concentrations ($[Na^+]_i$) (*bottom*) in the tetrodotoxin pretreatment. Tetrodotoxin ($30 \mu M$) was perfused from 3 to 4 min. Lidocaine was perfused at 7 min (1 mM). (B) The data of membrane potential (*top*) and $[Na^+]_i$ (*bottom*) in the tetrodotoxin pretreatment. Results are presented as mean \pm SEM; $n = 9$. * $P < 0.05$ compared with baseline values. # $P < 0.05$ compared with normal saline trials.

dose-dependent manner as compared with control (to $76 \pm 4\%$ at 0.1 mM, to $48 \pm 4\%$ at 1 mM; figs. 7A-C). However, the typical amount of membrane depolarization resulting from 1 mM lidocaine application (horizontal gray arrow), from the resting membrane potential in the control (shown as the I_{Na} at -60 mV in the control with black arrow) to the decreased membrane potential (usually -20 mV), should result in an inward sodium current (vertical gray arrow) (40-fold increase in I_{Na} between -60 and -20 mV).

Effects of Lidocaine on Steady State Activation Curve. Lidocaine did not apparently effect the steady state activation curve of I_{Na} . There was not a significant

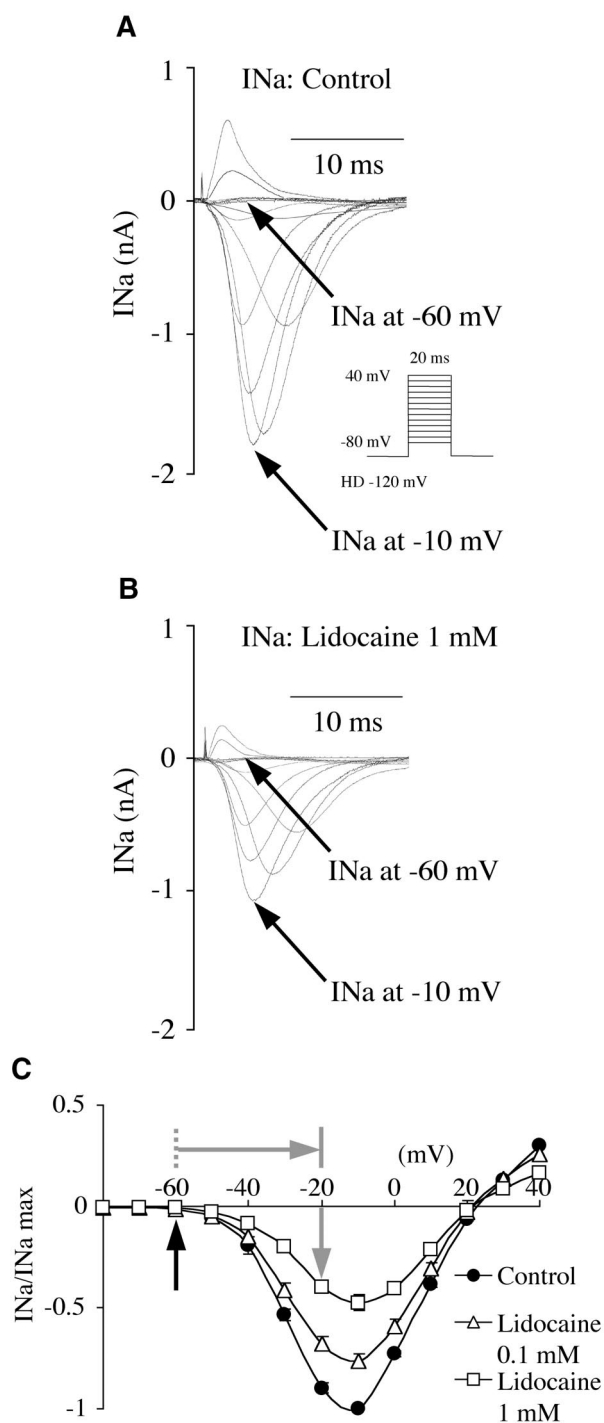


Fig. 7. (A) Current traces of control sodium currents (INa) in right pedal dorsal 1 neuron. Thirteen steps to potentials between -80 and $+40$ mV for 20 ms. (B) Current traces of INa after lidocaine (1 mM) perfusion. (C) Closed circles = current-voltage curves of INa in the control ($n = 7$); open triangles = 0.1 mM lidocaine perfusion ($n = 7$); open squares = 1 mM lidocaine perfusion ($n = 7$). Results are presented as mean \pm SEM. The black arrow shows the INa at resting membrane potential (-60 mV) in the control. The horizontal gray arrow shows the direction of membrane potential change from the resting level (-60 mV) to the potential after lidocaine (1 mM) perfusion. The vertical gray arrow highlights the inward sodium current generated by stepping the membrane potential to this depolarized potential of -20 mV, in patch clamp configuration.

shift of the steady state activation curve with up to 1 mM lidocaine (V_{50} : -24.2 mV at control to -22.3 mV at 0.1 mM, to -19.6 mV at 1 mM); also, there was no significant difference in the slope values up to 1 mM lidocaine (K value: 6.4 ± 0.3 at control to 6.5 ± 0.2 at 0.1 mM, to 7.3 ± 0.2 at 1 mM; figs. 8A-C).

Effects of Lidocaine on Steady State Inactivation Curve. Lidocaine induced a hyperpolarizing shift in the steady state inactivation curve in a dose-dependent manner (V_{50} : -55.3 mV at control to -62.3 mV at 0.1 mM, to -71.9 mV at 1 mM; K value: 8.6 ± 0.3 at control to 9.3 ± 0.3 at 0.1 mM, to 9.5 ± 0.3 at 1 mM; figs. 9A-C). With the perfusion of 1 mM lidocaine, 20% of the inward sodium current remained (approximately 80% inactivation) at the resting membrane potential of -60 mV (fig. 9C). From -60 to -20 mV, there are window currents where the activation and inactivation curves overlap, and thus a persistent inward sodium current can occur (slight conductance and incomplete inactivation) (fig. 10). Note that the range of this window current corresponds with the level of depolarization induced by 1 mM lidocaine (fig. 2B).

Discussion

Our results show that lidocaine increases $[Na^+]_i$ and depolarizes the membrane potential of the isolated RPeD1 respiratory pacemaker neuron at rest.

In the high- Na^+ saline trials, the increases in $[Na^+]_i$ after lidocaine treatment were significantly higher than that of normal saline. However, in the Na^+ -free saline trials, lidocaine did not produce an enhancement of $[Na^+]_i$. Therefore, the increase in $[Na^+]_i$ produced by lidocaine is likely from the extracellular fluid. These results indicate that the lidocaine-induced enhancement of $[Na^+]_i$ may result from the activation of Na channels. Consistent with this conclusion are our results that demonstrated that an increase in $[Na^+]_i$ induced by lidocaine was suppressed by hyperpolarization or after tetrodotoxin pretreatment. Therefore, one of the mechanisms by which lidocaine causes an increase in $[Na^+]_i$ may involve tetrodotoxin-sensitive voltage-dependent sodium channels. These results are supported by patch clamp data, which show that lidocaine increases INa approximately 40 times greater than observed at resting membrane potentials under control conditions.

In the current study, lidocaine decreased the maximum current response in a dose-dependent manner, and these data are consistent with those reported previously.³⁰⁻³² However, there were some variations with previous reports, one being that lidocaine increased inward sodium currents when compared with the INa of a resting membrane potential. This can be explained by analyzing previous reports where the effects of lidocaine on INa were compared at the same membrane potential.

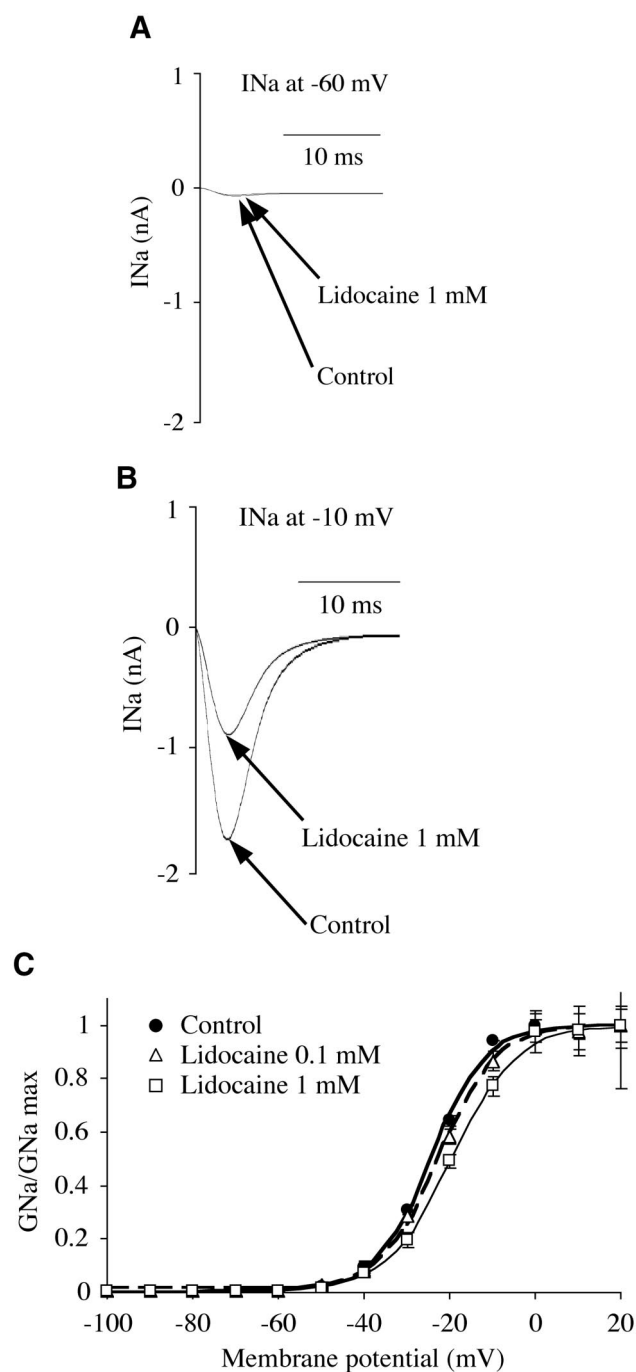


Fig. 8. (A) Current traces of control sodium currents (I_{Na}) and after lidocaine (1 mM) perfusion at -60 mV. (B) Current traces of I_{Na} control and after lidocaine (1 mM) perfusion at -10 mV. (C) Effects of lidocaine in steady state activation curve in right pedal dorsal 1 neuron normalized to the maximum I_{Na} in each group. Closed circles = control ($n = 7$); open triangles = 0.1 mM lidocaine perfusion ($n = 7$); open squares = 1 mM lidocaine perfusion ($n = 7$). Lines show the steady state activation curve fitted to Boltzmann relations. Thick line = control; dotted line = 0.1 mM lidocaine perfusion; thin line = 1 mM lidocaine perfusion.

For example, the I_{Na} was mostly compared at the membrane potential with an induced maximum current response of approximately -10 to 0 mV. However, there was in fact a difference in membrane potential before

and after lidocaine treatments. Therefore, we reason that the currents including I_{Na} must be compared for each membrane potential before and after lidocaine or after the blocker treatment. In addition, our results indicate that lidocaine depolarizes membrane potential, increases I_{Na} and induces more excitation to each neuron when the membrane potential is in the window currents. However, in contrast, when the membrane potential is high, outside of the window current, as would be the case during an action potential, lidocaine would decrease I_{Na} . In the steady state inactivation curve, lidocaine induced a hyperpolarizing shift, which is similar to that of previous reports.^{10,32,33} In these reports, it is concluded that the hyperpolarizing shift in the steady-state inactivation curve is one of the reasons that lidocaine reduces I_{Na} . However, in RPeD1, the availability of voltage-dependent sodium channels at -60 mV remains 20% after lidocaine perfusion (fig. 9C). In the range of -60 to -20 mV, which is the same range depolarized by 1 mM lidocaine (fig. 2B), activation and inactivation curves overlap before and after lidocaine perfusion, which is referred to as *window currents*. Therefore, in this range, depolarization induced by lidocaine will trigger conductance through sodium channels as activation occurs, and inactivation will be incomplete (fig. 10). Thus, depolarization of RPeD1 into the range of the window current allows for a small but persistent sodium influx with slower inactivation, which corresponds with the sodium imaging data of figure 2. In contrary, at maximum membrane potentials (> -10 mV), the availability of voltage-dependent sodium channels for persistent sodium influx is minimum, because inactivation is almost complete from -10 to $+20$ mV after a 5-s prepulse. This could be one of the reasons why lidocaine shows both inhibition and excitation in pacemaker neurons.

However, it is still unclear why lidocaine increases membrane potential. In the current study, lidocaine induced the hyperpolarizing shift in the steady state inactivation curve. Therefore, it is difficult to consider that I_{Na} through voltage-dependent sodium channels is the main cause of depolarization by lidocaine. Rodeau *et al.*⁹ reported that procaine (10 mM), another local anesthetic, increases membrane conductance and depolarizes membrane potential. This study concluded that local anesthetics increase membrane conductance by physically passing through channel pores. Procaine is an organic cation, but it moves through the cell membrane in "base" form, not "cation" form. Therefore, it is hard to consider that procaine will produce a major current itself. On the other hand, Ibuki *et al.*³⁴ reported that the intracellular concentrations of the ionic form of local anesthetics increased to approximately 70% of the extracellular concentration. Thus, depolarization of membrane potential by local anesthetics could be caused by an increase in the cation form of local anesthetics within the intracellular space or the gap between intracellular

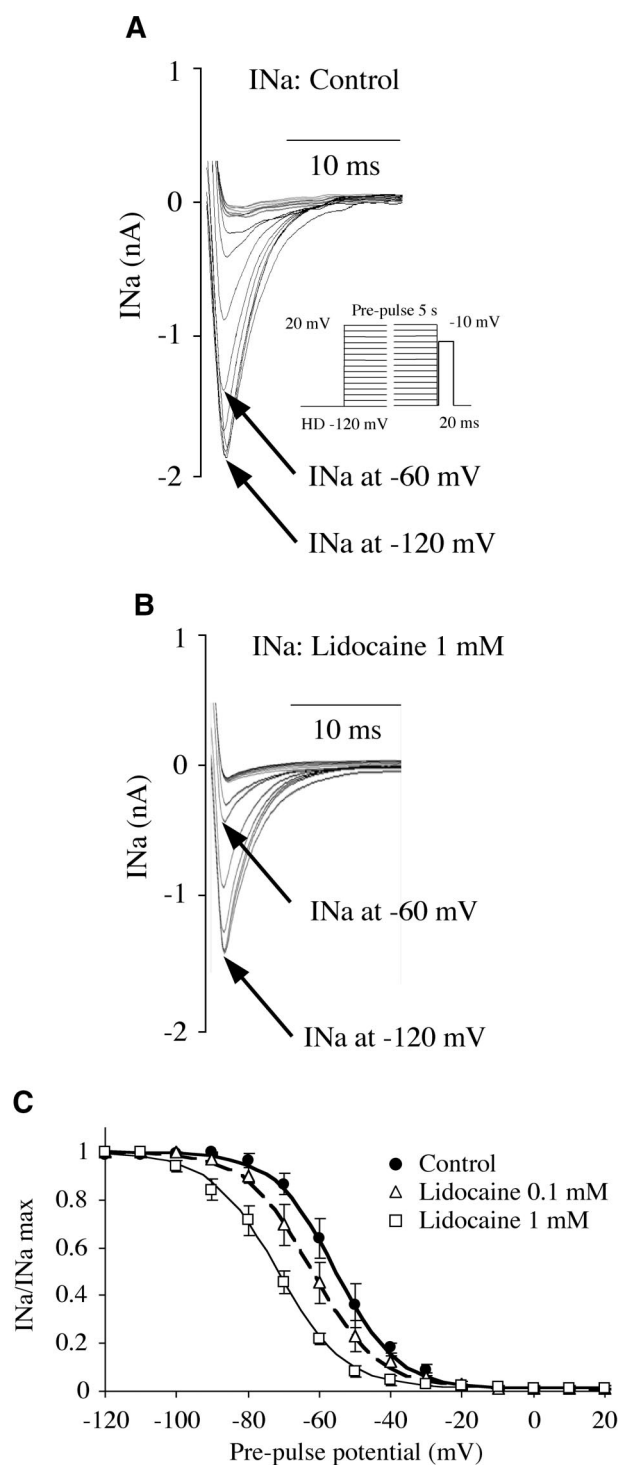


Fig. 9. (A) Current traces of control sodium currents (INa) in right pedal dorsal 1 neuron. INa was measured with a 20-ms test pulse to -10 mV after each prepulse of 17 steps from -120 to $+40$ mV with 10-mV increments for 5 s. (B) Current traces of INa after lidocaine (1 mM) perfusion. (C) Effects of lidocaine in steady state inactivation curve in right pedal dorsal 1 neuron normalized to the maximum INa in each group. Closed circles = control ($n = 7$); open triangles = 0.1 mM lidocaine perfusion ($n = 7$); open squares = 1 mM lidocaine perfusion ($n = 7$). Lines show the steady state inactivation curve fitted to Boltzmann relations. Thick line = control; dotted line = 0.1 mM lidocaine perfusion; thin line = 1 mM lidocaine perfusion.

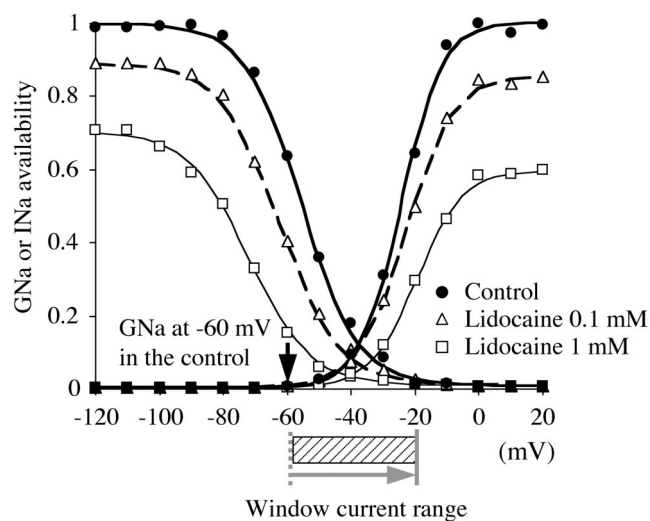


Fig. 10. Voltage dependence of activation and inactivation curves normalized to the maximum conductance or current of control group. Closed circles = control; open triangles = 0.1 mM lidocaine perfusion; open squares = 1 mM lidocaine perfusion. Lines show the steady state activation or inactivation curve fitted to Boltzmann relations. Shaded square shows the membrane potential range of the window current. Gray arrow shows the direction of membrane potential change from the resting membrane potential (-60 mV) to approximately -20 mV after 1 mM lidocaine perfusion.

and extracellular concentration of lidocaine. Our results indicate that lidocaine also depolarized membrane potential when sodium was excluded from the extracellular fluid. However, this depolarization was significantly less than that in normal saline trials. Also, tetrodotoxin pretreatment suppressed membrane depolarization by lidocaine. These results indicate that the lidocaine-induced depolarization of the membrane potential is not solely generated by lidocaine itself, but that Na^+ influx via the tetrodotoxin-sensitive, voltage-dependent sodium channels promotes this depolarization. Komai and McDowell³⁵ reported that local anesthetics inhibit potassium currents and induce depolarization. This also may contribute to the initial membrane depolarization; however, potassium currents were not included in this study.

We choose concentrations of 0.01–1 mM lidocaine in the study because it is reported that lidocaine at doses of 0.07–0.1 mM of blood concentration induce convulsions in humans.³⁶ In this study, we used SBFI-AM to measure $[\text{Na}^+]_i$. To investigate the interference to SBFI-AM by *Lymnaea* saline and lidocaine, we measured the fluorescent ratio using the same concentration of SBFI and lidocaine solution, but no major interference or fluorescent loss was observed. In figure 2, the depolarized membrane potential by lidocaine only lasts 3–4 min and then has a tendency to come back to the base level even during the application of lidocaine. Many factors contribute to the maintaining of membrane potential; thus, the inhibitory effect of lidocaine on voltage-dependent sodium channels may not directly result in alternations in

membrane potential. Other factors, such as sodium-calcium exchangers and other ionic currents, may be modified by lidocaine application. To determine how lidocaine changes $[Na^+]_i$, more investigations that include these exchangers and sodium channels are necessary. The major receptors and ion channels that have been identified in *L. stagnalis* are similar to those found in humans, and therefore, *L. stagnalis* represents an excellent model to study the effects of lidocaine.

In conclusion, lidocaine increases intracellular sodium concentration and promotes excitation in respiratory pacemaker neurons through voltage-dependent sodium channels by altering membrane potential. This depolarization is enough to activate a persistent sodium influx through the window current, an idea confirmed with sodium imaging.

The authors thank Tyler Dunn, Ph.D. (Respiratory and Neuroscience Research Groups, Departments of Cell Biology and Anatomy/Physiology and Biophysics, Faculty of Medicine, University of Calgary, Calgary, Alberta, Canada), and Naweid I. Syed, M.D., Ph.D. (Associate Professor, Respiratory and Neuroscience Research Groups, Departments of Cell Biology and Anatomy/Physiology and Biophysics, Faculty of Medicine, University of Calgary), for helping with the manuscript preparation.

References

1. Tanaka K, Yamasaki M: Blocking of cortical inhibitory synapses by intravenous lidocaine. *Nature* 1966; 209:207-8
2. Jordan E, Kee R, Yim G: The effects of lidocaine in the cerebral cortex. *ANESTHESIOLOGY* 1971; 34:327-32
3. Seo N, Oshima E, Stevens J, Mori K: The tetraphasic action of lidocaine on CNS electrical activity and behavior in cats. *ANESTHESIOLOGY* 1982; 57:451-7
4. Wasgman I, Jong R, Prince D: Effects of lidocaine on the central nervous system. *ANESTHESIOLOGY* 1967; 28:155-72
5. Nestler E, Hyman S, Malenka R: Chapter 3, Electrical Excitability of Neurons. Edited by Nestler E. New York, McGraw-Hill, 2001, pp 33-58
6. Levitan IB, Kaczmarek LK: Membrane ion channels and ion currents, *The Neuron*, 3rd edition. Oxford University Press, 2002, pp 67-87
7. Baartscheer A, Schumacher CA, Fiolet JW: Cytoplasmic sodium, calcium and free energy change of the Na^+/Ca^{2+} -exchanger in rat ventricular myocytes. *J Mol Cell Cardiol* 1998; 30:2437-47
8. Bernardi GK, Mercuri GK: Hyperpolarization induces a rise in intracellular sodium concentration in dopamine cells of the substantia nigra pars compacta. *Eur J Neurosci* 1998; 10:1926-9
9. Rodeau JL, Flament S, Browaeys E, Vilain JP: Effect of procaine on membrane potential and intracellular pH in *Xenopus laevis* oocytes. *Mol Membrane Biol* 1998; 15:145-51
10. Castaneda-Castellanos DR, Nikonov I, Kallen RG, Pinto ER: Lidocaine stabilizes the open state of CNS voltage-dependent sodium channels. *Molecular Brain Res* 2002; 99:102-13
11. Syed N, Bulloch A, Lukowiak K: In vitro reconstruction of the respiratory central pattern generator of the mollusk *Lymnaea*. *Science* 1990; 12:282-5
12. Pennartz CM, Bierlaagh MA, Geurtsen AM: Cellular mechanisms underlying spontaneous firing in rat suprachiasmatic nucleus: Involvement of a slowly inactivating component of sodium current. *J Neurophysiol* 1997; 78:1811-25
13. Rota M, Vassalle M: Patch-clamp analysis in canine cardiac Purkinje cells of a novel sodium component in the pacemaker range. *J Physiol* 2003; 548:147-65
14. Gilly WF, Gillette R, McFarlane M: Fast and slow activation kinetics of voltage-gated sodium channels in molluscan neurons. *J Neurophysiol* 1997; 77:2373-84
15. Staras K, Györfi J, Kemenes G: Voltage-gated ionic currents in an identified modulatory cell type controlling molluscan feeding. *Eur J Neurosci* 2002; 15:109-20
16. Branes S, Syed NI, Bulloch GM, Lukowiak K: Modulation of ionic currents by dopamine in an interneuropore of the respiratory central pattern generator of *Lymnaea stagnalis*. *J Exp Biol* 1994; 189:37-54
17. Hamakawa T, Feng ZP, Grigoriv N, Inoue T, Takasaki M, Roth S, Lukowiak K, Hasan SU, Syed NI: Sevoflurane induced suppression of inhibitory synaptic transmission between soma-soma paired *Lymnaea* neurons. *J Neurophysiol* 1999; 82:2812-9
18. Spencer GE, Syed NI, Lukowiak K, Winlow W: Halothane-induced synaptic depression at both in vivo and in vitro reconstructed synapses between identified. *Lymnaea Neurons* 1995; 74:2604-13
19. Woodall AJ, Naruo H, Prince DJ, Feng ZP, Winlow W, Takasaki M, Syed NI: Anesthetic treatment blocks synaptogenesis but not neuronal regeneration of cultured *Lymnaea* neurons. *J Neurophysiol* 2003; 90:2232-9
20. Minta A, Tsien RY: Fluorescent indicators for cytosolic sodium. *J Biol Chem* 1989; 32:19449-57
21. Despa S, Islam MA, Pogwizd SM, Bers DM: Intracellular $[Na^+]_i$ and Na^+ pump rate in rat and rabbit ventricular myocytes. *J Physiol* 2002; 15:133-43
22. Tsubokawa H, Miura M, Kano M: Elevation of intracellular Na^+ induced by hyperpolarization at the dendrites of pyramidal neurones of mouse hippocampus. *J Physiol* 1999; 517:135-42
23. Borin M, Siffert W: Stimulation by thrombin increases the cytosolic free Na^+ concentration in human platelets. *J Biol Chem* 1990; 265:19543-50
24. Knopfel T, Anchisi D, Alojado ME, Tempia F, Strata P: Elevation of intradendritic sodium concentration mediated by synaptic activation of metabotropic glutamate receptors in cerebellar Purkinje cells. *Eur J Neurosci* 2000; 12:2199-204
25. Diarra A, Sheldon C, Church J: In situ calibration and $[H^+]$ sensitivity of the fluorescent Na^+ indicator SBFI AJP-cell. *Physiology* 2000; 280:1623-33
26. Brussaard AB, Maat AT, Vlieger TA, Kits KS: Inhibitory modulation of neuronal voltage-dependent sodium current by Phe-Met Arg-Phe amide. *Neurosci Lett* 1990; 111:325-32
27. Brussaard AB, Lodder JC, Maat AT, Vlieger TA, Kits KS: Inhibitory modulation by FMRFamide of the voltage-gated sodium current in identified neurons in *Lymnaea stagnalis*. *J Physiol* 1991; 441:385-404
28. Ogata N, Tatebayashi H: Kinetic analysis of two types of Na^+ channels in rat dorsal root ganglia. *J Physiol* 1993; 466:9-37
29. Tabarean IV, Narahashi T: Kinetics of modulation of tetrodotoxin-sensitive and tetrodotoxin-resistant sodium channels by tetramethrin and deltamethrin. *J Pharmacol Exp Ther* 2001; 299:988-97
30. Strichartz GR: Neural physiology and local anesthetic action, *Neural Blockade*. Edited by Cousins MJ, Bridenbaugh PO. New York, Lippincott-Raven, 1998, pp 35-54
31. De Jong RH: Local anesthetic pharmacology, *Regional Anesthesia and Analgesia*. Edited by Brown DL. Philadelphia, WB Saunders, 1996, pp 125-42
32. Nuss HB, Kambouris NG, Marban E, Tomaselli GF, Balser JR: Isoform-specific lidocaine block of sodium channels explained by differences in gating. *Biophys J* 2000; 78:200-10
33. Vedantham V, Cannon SC: The position of the fast-inactivation gate during lidocaine block of voltage-gated Na^+ channels. *J Gen Physiol* 1999; 113:7-16
34. Ibusuki S, Katsuki H, Takasaki M: The effects of extracellular pH with and without bicarbonate on intracellular procaine concentrations and anesthetic effects in crayfish giant axons. *ANESTHESIOLOGY* 1998; 88:1449-57
35. Komai H, McDowell TS: Local anesthetic inhibition of voltage-activated potassium currents in rat dorsal root ganglion neurons. *ANESTHESIOLOGY* 2001; 94:1089-95
36. Mercedes C: Acute complication and side effects of regional anesthesia, *Regional Anesthesia and Analgesia*. Edited by Brown D. Philadelphia, WB Saunders, 1996, pp 446-61